JOURNAL OF Materials CHEMISTRY

The synthesis, mesomorphism and mesophase structure of anisotropic imines and their complexes with rhenium(I)

Xiao-Hua Liu,[a,b] Benoît Henirich,[c] Ian Manners,[b] Daniel Guillon[c] and Duncan W. Bruce*[a]

[a]*School of Chemistry, University of Exeter, Stocker Road, Exeter, UK EX4 4QD. Fax: +44 1392 263434. E-mail: d.bruce@exeter.ac.uk*
[b]*Department of Chemistry, University of Toronto, Toronto, M5S 3H6, Canada*
[c]*IPCMS, Groupe des Materiaux Organiques, 23 rue du Loess, BP 20CR, 67037 Strasbourg cedex, France*

Received 11th October 1999, Accepted 20th December 1999

Highly anisotropic imine ligands have been synthesised and complexed to Re(I). Two series of ligands and complexes were obtained with various chain lengths, showing smectic and nematic phases for the ligands and only a nematic phase for the complexes. The identity of the crystal smectic phase in the ligands was studied by X-ray diffraction and identified as a crystal J phase.

Introduction

For some time, derivatives of ferrocene (and some of ruthenocene) were the sole examples of formally six-coordinate, rod-like molecules which formed liquid crystal mesophases,[1] with the vast majority of literature on calamitic metal complexes concentrating on 2- and 4-coordinate complexes of metals taken from Groups 9–11.[2] Informed by these studies on ferrocene-based mesogens, we began to search for rational means by which high coordination number metal centres could be used successfully as the basis for the construction of calamitic materials. In 1994, we reported[3] that complexation of strongly mesomorphic imines to Mn(I) centres *via* orthometallation led to mesomorphic octahedral metal complexes with a rod-like shape (**1**, Fig. 1). The design of these materials was based on the premise that if a large structural perturbation (*i.e.* 6-coordinate metal centre) were to be tolerated in a mesogen, then the organic part would need to be sufficiently anisotropic to withstand such disruption. The strategy was successful and the manganese complexes demonstrated a nematic mesophase in the range 120–190 °C.

One of the problems sometimes encountered in the study of mesomorphic metal complexes is the lack of thermal stability of the materials at the clearing point, which can be a significant drawback in the study of their physical properties. In order to circumvent this problem, the first strategy to obtain more stable materials was to modify the ligand to access lower melting systems to see how a change in the ligand can affect the thermal parameters. First of all, removing an aromatic group to form

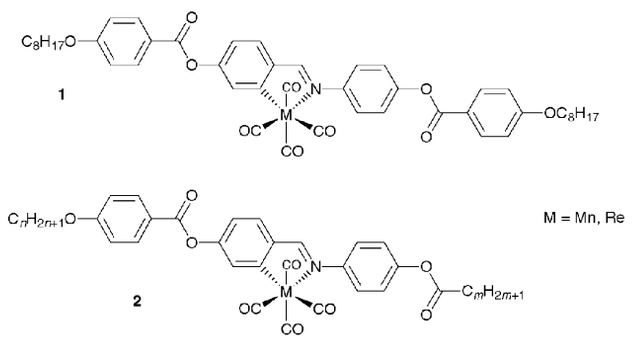

Fig. 1 Structures of mesomorphic complexes of Mn(I) and Re(I).

complex **2** (Fig. 1) led to alkanoyloxy-substituted materials which show monotropic nematic phases.[4] All of the alkanoyloxy substituted complexes melted in the range 100–124 °C, giving mesophases in the range 63–83 °C. As a second strategy, we decided to synthesise the related complexes of rhenium(I) on account of the fact that metal complexes of 3rd row transition elements are often much more stable than their 2nd or 1st row counterparts. This strategy proved successful and we reported the fact in a communication.[4] In the present paper, we now report a systematic investigation of the synthesis and mesomorphism of two series of rhenium(I) complexes and their precursor ligands to examine properly the effect that the ligand can have on the mesomorphism of the complexes.

Preparation of the ligands and complexes

The ligands were prepared as follows and as shown in Scheme 1. 4-Alkoxybenzoic acid was esterified (using DCC and DMAP) with 4-hydroxybenzaldehyde to give 4-alkoxybenzoyloxy-4′-benzaldehyde (**3**), and with 4-nitrophenol to give 4-alkoxybenzoyloxy-4′-nitrobenzene (**4**). Reduction of the nitrophenyl ester with tin(II) chloride at reflux in ethanol led to the related amine (**5**). The target ligands (**6**, **7**) were then obtained in a Schiff base condensation in toluene at room temperature using a catalytic quantity of acetic acid. Yields for the esterification reaction were typically above 80%, while the Schiff base condensation gave yields of 75–90%. Reduction of the nitro group typically proceeded in yields of around 75%. In addition, two ligands were synthesised with a *trans*,*trans*-4-alkylcyclohexanoyloxy ring using exactly the same approach. The complexes (**8**, **9**) were subsequently obtained in yields of 75–85% by reaction of the ligand with $[ReMe(CO)_5]$[5] in toluene at reflux, followed by purification by column chromatography.

Complexation was evident from spectroscopy. Thus, in the ^1H NMR spectra of the ligands, the imine proton shifted from δ 8.45 in the ligand to δ 8.62 in the complex and the AA′XX′ spin system of one ring changed to an AMX system on complexation. Further, the complexes showed CO stretching vibrations at 2092, 1991, 1987 and 1934 cm^{-1} compared with 2129, 2012 and 1975 cm^{-1} for $[ReMe(CO)_5]$. All the new Re complexes were characterized by elemental analysis, infrared spectroscopy, ^1H and $^{13}C\{^1H\}$ NMR spectroscopy and by 2-D NMR experiments.

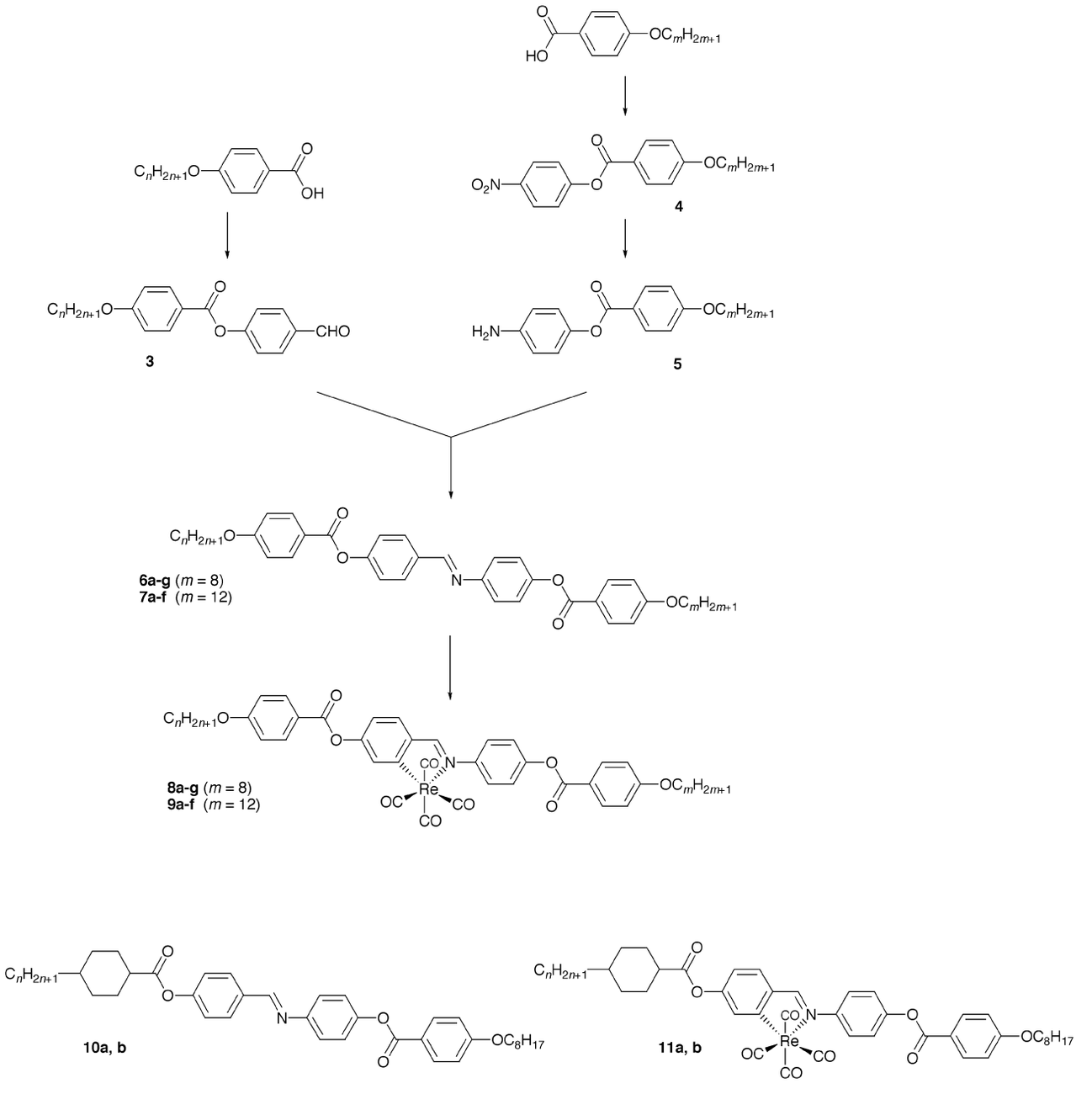

Scheme 1

Mesomorphic properties of the ligands

Two series of ligands were prepared. In the first (**6**), one chain length was fixed ($m=8$), while the other chain length was varied ($n=5$, 6, 7, 8, 10, 12, 14), while in the second series (**7**), the same chain was fixed at a longer length ($m=12$) with the other chain again being varied ($n=5$, 6, 7, 10, 2, 14).

The mesomorphism of both series was similar and is summarised in Table 1 and Fig. 2 and 3. Both series of ligands had rather high transition temperatures with clearing points in excess of 260 °C, consistent with the highly anisotropic nature of the ligand which we had initially reasoned was needed to preserve mesomorphism when the metal tetracarbonyl group was introduced.

The ligands **6** showed a high-temperature nematic phase above a wide-range smectic C phase. The stability of the nematic phase fell from around 320 °C at the shortest chain length (**6a**, $n=5$) to about 260 °C for the longest chain length (**6g**, $n=14$), while the smectic C phase stability increased from around 120 to 220 °C for the same range of chain lengths. All homologues showed a crystal smectic phase below the smectic C phase, and as the stability of this phase was largely constant although it fell slightly for the longest chain lengths, then the range of the smectic C phase increased from 35 to 188 °C across the phase diagram. Curiously, one homologue (**6f**, $n=12$) showed a smectic I phase over a range of 8 °C. The homologue with $n=8$ (**6d**) was originally reported in our preliminary communication where we identified the crystal smectic phase as a G phase, whereas in Table 1, we now assign it as a crystal J phase. The original assignment was based solely on optical microscopy, whereas the assignment as a J phase is based on the results of detailed X-ray crystallography which is reported below.

For the ligands **7** with the longer fixed chain length, there was a similar pattern of behaviour, although some differences were evident. First, while the clearing points of ligands **7** were 10–20 °C lower than those of **6**, the melting points were similar. Further, the longer chain length stabilised the smectic C phase at the expense of the nematic phase by around 40 °C for the smallest values of m and around 10 °C for larger values, leading

Table 1 Thermal behaviour of ligands **6**, **7** and **10**

	n	Transition	*T*/°C	ΔH/kJ mol^{-1}	ΔS/J K^{-1} mol^{-1}
6a	5	Crys–J	106	25.1	66
		J–S_C	119	4.5	12
		S_C–N	154	0.8	2
		N–I[a]	322	—	—
6b	6	Crys–J	101	20.1	54
		J–S_C	113	3.9	10
		S_C–N	167	1.3	3
		N–I[a]	318	—	—
6c	7	Crys–J	106	20.4	54
		J–S_C	118	3.8	10
		S_C–N	183	1.8	3
		N–I[a]	302	—	—
6d	8	Crys–J	116	25.2	65
		J–S_C	124	3.8	10
		S_C–N	202	1.9	4
		N–I[a]	298	2.2	4
6e	10	Crys–J	112	22.1	57
		J–S_C	119	1.0	3
		S_C–N	215	3.0	6
		N–I[a]	294	3.1	5
6f	12	Crys–J	91	13.5	38
		J–S_I	110	0.4	1
		S_I–S_C	118	0.8	2
		S_C–N	224	1.4	3
		N–I[a]	284	1.0	1
6g	14	Crys–J	88	36.0	100
		J–S_C	99	1.2	3
		S_C–N	217	1.3	3
		N–I[a]	262	—	—
7a	5	Crys–J	107	16.7	44
		J–S_C	111	1.5	4
		S_C–N	193	1.2	3
		N–I[a]	298	—	—
7b	6	Crys–J	104	32.9	87
		J–S_I	111	0.4	1
		S_I–S_C	114	1.1	3
		S_C–N	208	1.7	4
		N–I[a]	290	—	—
7c	7	Crys–J	95	16.2	44
		J–S_I	106	0.4	1
		S_I–S_C	113	1.3	3
		S_C–N	213	1.8	4
		N–I	289	1.9	3
7d	10	Crys–J	95	29.8	81
		J–S_I	103	0.3	1
		S_I–S_C	115	1.7	4
		S_C–N	226	3.6	7
		N–I[a]	271	2.0	4
7e	12	Crys–J	99	32.6	88
		J–S_I	105	0.1	0
		S_I–S_C	113	1.0	3
		S_C–N	234	3.3	7
		N–I	269	1.8	3
7f	14	Crys–S_I	99	36.7	99
		S_I–S_C	117	1.9	5
		S_C–N	239	5.5	11
		N–I	266	2.4	4
10a	5	Crys–J	83	27.2	76
		J–S_C	131	3.7	9
		S_C–N	191	0.9	2
		N–I	299	0.9	2
10b	7	Crys–J	87	33.7	94
		J–S_I	137	0.6	1
		S_I–S_C	143	1.7	4
		S_C–N	216	1.0	2
		N–I	307	1.7	3

[a]Clearing points were observed using a polarizing optical microscope.

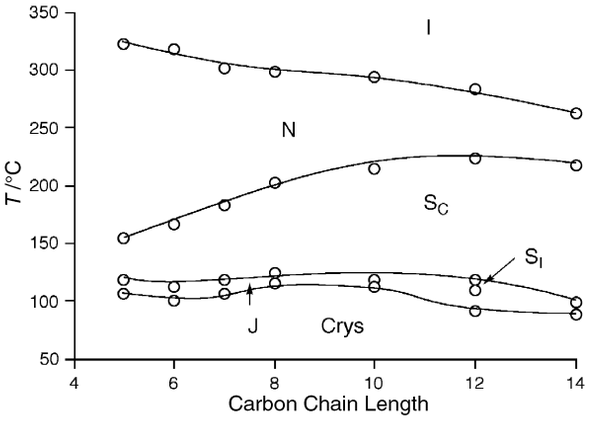

Fig. 2 Phase diagram for ligands **6**.

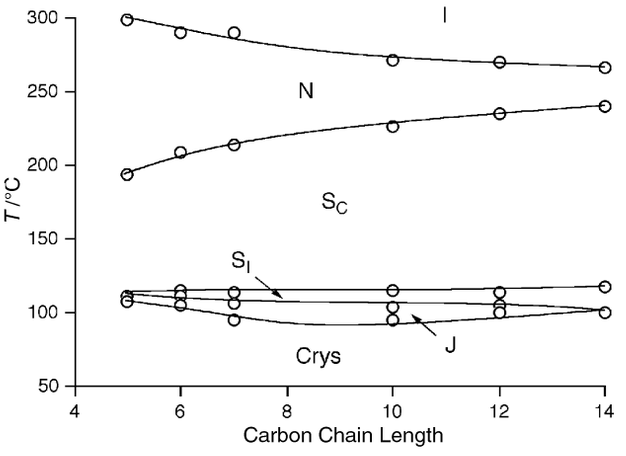

Fig. 3 Phase diagram for ligands **7**.

to a reduced nematic range in **7**. Similarly, while the crystal smectic phase persisted in all but the longest chain homologue, this time the S_I phase was present in all homologues except that with the shortest chain length showing that longer chains were also stabilising S_I.

All fluid phases of both **6** and **7** were identified by their characteristic optical textures, with the 'fingerprint' texture being seen at the S_C–N transition. The S_I phase gave a schlieren texture which was rather difficult to bring into focus.[6]

Finally, and for completion, we note the thermal behaviour of two other ligands which were reported in our initial communication on the manganese complexes.[3] Thus, the two alkylcyclohexyl derivatives (**10a** and **10b**) were reported as having nematic, smectic C and a crystal smectic G in the former case, and a nematic, smectic C, smectic I and crystal J phase in the latter. Assignments of the crystal phases were on the basis of optical microscopy alone, although in the light of the studies reported below, we would now assign both crystal phases as crystal smectic J. While overall the transition temperatures are rather similar to those observed for the related ligands with alkoxyphenyl groups, we would note that the S_C phase in **10** is much less stable than in either **6** or **7** which may well be related to the greater motion possible with the flexible cyclohexyl group disrupting the lamellar arrangement.

The identity of the crystal smectic phase

In our initial communication on the mesomorphism of orthometallated imine complexes of Mn(I), we reported the behaviour of the ligand **6d** ($n=m=8$) and identified the crystal smectic phase as a crystal smectic G on the basis of optical microscopy. However, in the present work, we found it

increasingly difficult to assign the crystal smectic phase seen in many derivatives as either G or J on the basis of microscopy alone, and so we undertook a detailed study by X-ray diffraction in order to resolve the question. In total, five complexes were studied and they were chosen as examples where the crystal smectic phase was formed either directly from a smectic C phase or from a smectic I phase.

First, it was possible to confirm the existence of a smectic C phase due to the presence of two sharp reflections in the ratio 1 : 2 in the small angle region corresponding to a lamellar system. The measured layer spacing was about 50% of the calculated molecular length suggesting a tilt angle of around 50° in all examples studied. In the case of the smectic I phase, in addition to the reflections at small angle, there was, in the wide angle region, a slightly broad reflection from the packing of the rigid cores which overlapped with the diffuse 4.5 Å reflection due to the packing of the molten alkyl chains. The width of this peak strongly supported the assignment as S_I as it is normally the case that the reflection from the packing of the cores would be broader if the phase were S_F.[7]

The X-ray diffraction pattern for the crystal smectic phase showed (Fig. 4), at wide angle, a diffuse reflection due to the packing of the alkyl chains, an intense, first order reflection due to the two-dimensional hexagonal packing of the rigid cores and several other sharp reflections of low intensity corresponding to an (*hkl*) indexation with $h \neq 0$ and/or $k \neq 0$ and $l \neq 0$. In order to identify the phase, both a crystal smectic G and a crystal smectic J monoclinic lattice were considered (Fig. 5), with *a* and *b* being placed within, and normal to, the tilt plane, respectively. It was considered that there were two molecules per unit cell and unit cell angles of $\alpha = \gamma = 90°$, $\beta \neq 90°$ were assumed.

From the location of the (*hkl*) satellite reflections relative to the first order (*hk*0) reflection of the hexagonal packing, the angle β and therefore the other cell parameter and cell volume (V_c) are readily deduced (Table 2). The largest values for V_c and *c* correspond to the crystal J lattice and the smallest to the crystal G lattice; intermediate values would be found for a crystal smectic M type of lattice (an analogue of the crystal G and J phases in which the tilt direction is somewhere between that found in these two phases)[8] with any other orientation of the crystallographic axes with respect to the tilt plane (Fig. 5c). The corresponding molecular volumes $V_m = V_c/2$ (recall that two molecules per unit cell are proposed) and cell parameters *c* are plotted against the sum of the carbon chain lengths $n+m$ (oxygen being included in the rigid core for these purposes) and compared to the calculated molecular volume, V_m, and the molecular lengths *l* (Fig. 6; V_m being obtained from the well known volume of molten aliphatic tails, from the transverse area of the rigid core σ_0 deduced from the spacing of the (*hk*0) reflection and from the rigid core length deduced from molecular modelling). It is then clear that the lattice parameters which are found by assuming a crystal smectic G type of monoclinic lattice lead to a cell volume which is too small with respect to the volume of the 2 molecules contained in the monoclinic lattice. In contrast, the cell volume is in good agreement with that calculated with the lattice parameter obtained for a crystal smectic J type of monoclinic lattice. This suggests that the arrangement is of the smectic J type or close to it, suggesting that all samples exhibit a crystal J phase.

One particular feature of interest was found in sample **6e** (Fig. 7) which was very different from that in the other samples, namely the occurrence of an additional, low-intensity (12) reflection. In the case of a truly centred arrangement in the *ab* plane, this reflection would be extinguished, but its presence suggests that there must be a shift along *c* between adjacent rows of molecules parallel to the tilt plane. However, an alternative explanation, which cannot be excluded, is that α is in fact not exactly equal to 90° so that the lattice is actually that of a crystal smectic M phase (*i.e.* a quasi-crystalline J lattice).

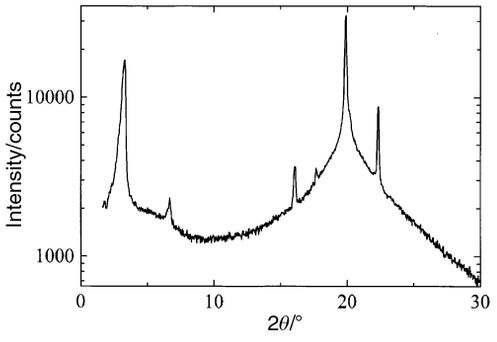

Fig. 4 X-Ray diffraction pattern for **6a** at 115 °C.

Influence of chain length and temperature

The variation of *d* with *T* is less than 0.01% °C^{-1} within a phase domain, with the transitions from the S_C to the S_I phase and from the S_I to the J phase being associated with jumps in *d* of the order of 1% in the former case, there being no jump in the latter. This corresponds to molecular areas, *S*, increasing slightly with increasing *T* and decreasing $n+m$ (Fig. 8). The tilt angle, ψ, which is deduced from the ratio of *S* and of the transverse area to the rigid part σ_0 (obtained from the spacing corresponding to the (*hk*0) reflection in the case of the S_I and J phases and evaluated from the location of the diffuse reflection in the wide-angle region in the case of the S_C phase) lies in the range 50° to 55°, with a tendency to decrease with increasing $n+m$ (Fig. 9). It is quasi-independent of temperature in the J and S_I phases, and only a few degrees larger in the S_C phase (Fig. 10).

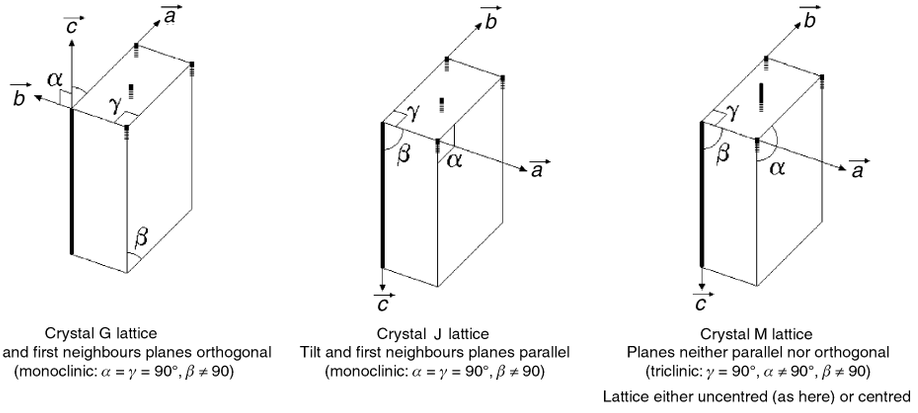

Fig. 5 Illustration of the relationships between the crystal G, J and M lattices.

Table 2 Parameters for putative crystal G and J lattices

$2\theta_o$/°	d_{obs}/Å	I	G phase: (hkl)	J phase: (hkl)	$2\theta_{calc}$/°	d_{calc}/Å
2.55	34.6	vs	001	001		
19.91	4.46	vs	200/110	110/020	19.91	4.46
21.72	4.09	w	20$\bar{1}$	11$\bar{1}$	21.74	4.08
18.25	4.86	w	201	111	18.27	4.85
16.89	5.24	vw	202	112	16.87	5.25

	a/Å	b/Å	c/Å	β/°	l/Å	D^c/Å	σ_0/Å^2	ψ/°	S/Å^2	V_m/10^3 Å^2
G lattice:	12.0	5.14	46.6	47.8	c	b	22.9	42.2	30.9	1.07
J lattice:	8.14	8.91	54.7	39.2	c	b	22.9	50.8	36.3	1.25

$\sigma_0 = d_{200}b$; $\psi = 90 - \beta$; $S = (ab)/2 = \cos\psi$; $V_m = d_{001}S$.

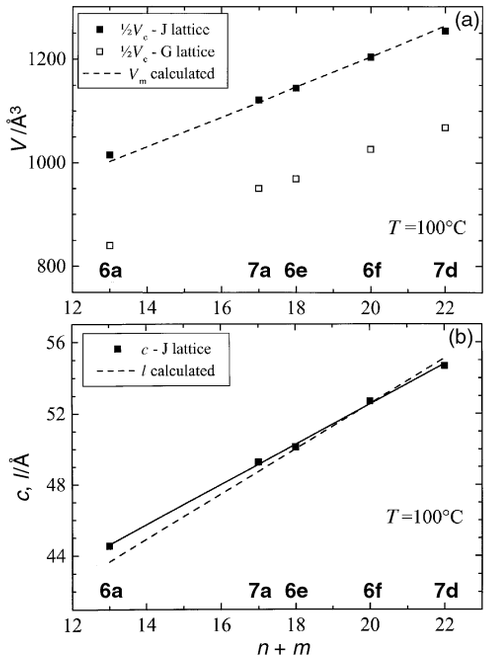

Fig. 6 Plot of (a) calculated molecular volume and (b) lattice c parameter against total chain length.

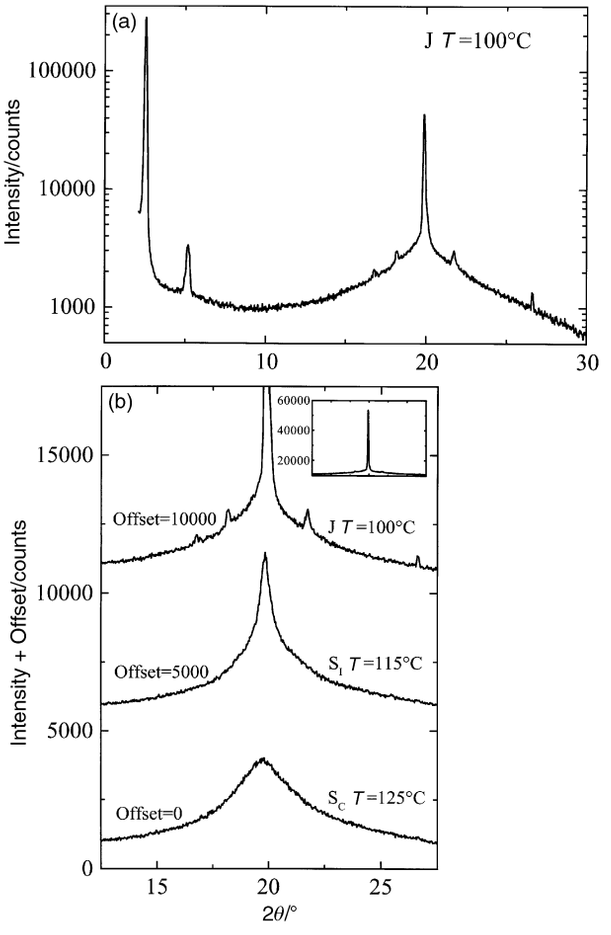

Fig. 7 X-Ray diffraction patterns for **6e** at 100 °C: (a) full pattern; (b) wide angle region.

Mesomorphic properties of the complexes

The mesomorphism of the two series of Re(I) complexes, **8** and **9** formed from ligands **6** and **7**, respectively was evaluated and compared with that of examples which we had described previously. Thermal data are collected in Table 3 and are displayed in Fig. 11 and 12.

In broad terms, the mesomorphism of all of the rhenium complexes was the same, melting to a nematic phase in the range 130–155 °C and clearing between 140 and 198 °C. Interestingly, while it was found that lower clearing points (10–20 °C) were found for complexes **9** (m=12) compared to complexes **8** (m=8), no such dependence of the melting point was observed. Further, the decrease in T_{NI} as a function of chain length was similar in both the ligands and the complexes as illustrated in Fig. 13. The two complexes derived from the alkylcyclohexyl ligands (**11a** and **11b**) also showed only a nematic phase although it was interesting that both the melting and clearing points were lower by some 20–30 °C compared with the related alkoxyphenyl complexes. By analogy with studies on related complexes,[9] we attribute this to the removal of the oxygen of the alkoxy group and the attendant, stabilising, molecular dipoles. It is important to note here that we found reproducible mesomorphism after several heat–cool cycles, demonstrating the thermal stability of these

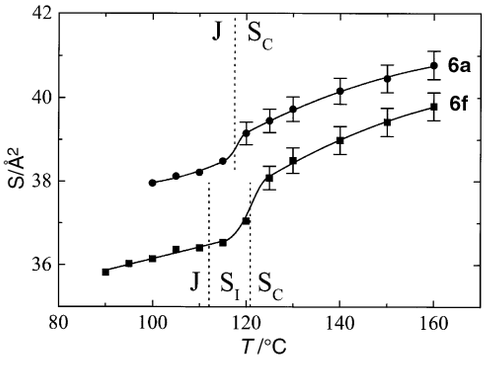

Fig. 8 Plot of molecular area, S, as a function of temperature for **6a** and **6e**.

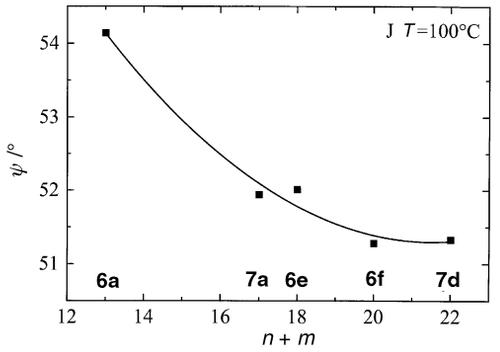

Fig. 9 Plot of tilt angle (ψ) against total chain length at 100 °C in the crystal J phase.

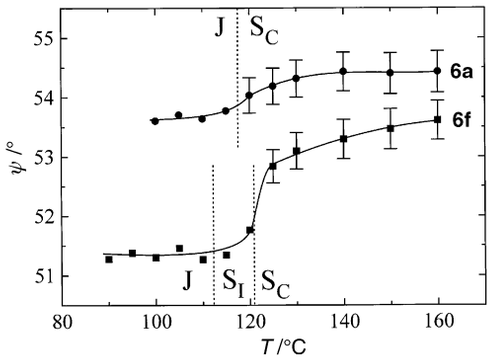

Fig. 10 Plot of tilt angle as a function of temperature for **6a** and **6e**.

materials which is in contrast to their manganese congeners which decompose on clearing.

The fact that, on complexation, the mesomorphism changes from nematic and smectic phases solely to nematic is something we have discussed elsewhere on several occasions[3,4,9] and results from the reduction in ligand anisotropy on the introduction of the [Re(CO)$_4$] group. It is, however, interesting that even at the longest chain lengths shown ($n+m=26$) there is no sign of a smectic phase, although we have recently found that smectic phases can be induced in the complexes, but only on the introduction of *two* fluorocarbon chains.[10]

However, an interesting comparison arises when we look at the mesomorphism of these complexes in relation to other octahedral Re(I) complexes of diazabutadiene (**12**)[11] and 2,2′-bipyridine (**13**)[12] ligands (Fig. 14). In these last complexes, it is a [ReX(CO)$_3$] fragment which binds to a neutral ligand and, in almost all cases, the melting and clearing points are not substantially reduced, in many cases increasing on complexation. However, contrast this with the Re(I) imine complexes where clearing points drop substantially compared to those of the ligands. While the complexes of the diazabutadienes may perhaps be regarded slightly differently as they exhibit a bent structure due to the formation of a five-membered ring on complexation (although we see no real evidence of so-called 'banana' phases), the bipyridine complexes are more similar and we can regard the [ReX(CO)$_3$] fragment as a structural perturbation in the same way that we discussed the [Re(CO)$_4$] fragment above in relation to the imine systems. Why then does one fragment lower the clearing points of its ligands (imine complexes) and yet raise them in others (diazabutadienes and bipyridines)?

As yet, we do not know the answer to this question although it is under investigation. However, one possible explanation relates to the fact that in the case of the diazabutadiene and bipyridine ligands, there are two lateral dipolar functions around the metal centre, namely a *cisoid* diimine function and a Re–X bond. We believe that these may have some significance in determining the behaviour in these systems and are currently pursuing this line of investigation.

Table 3 Thermal behaviour of complexes **8**, **9** and **11**

	n	Transition	T/°C	ΔH/kJ mol^{-1}	ΔS/J K^{-1} mol^{-1}
8a	5	Crys–N	155	37.2	87
		N–I	198	1.4	3
8b	6	Crys–N	159	42.5	98
		N–I	191	1.7	4
8c	7	Crys–N	150	41.0	97
		N–I	182	1.2	3
8d	8	Crys–N	154	32.2	75
		N–I	176	1.2	3
8e	10	Crys–N	128	29.0	72
		N–I	166	1.5	3
8f	12	Crys–N	130	48.0	118
		N–I	164	0.9	2
8g	14	Crys–N	131	51.3	127
		N–I	152	1.3	3
9a	5	Crys–N	150	41.1	98
		N–I	172	1.4	3
9b	6	Crys–N	160	55.2	128
		N–I	169	1.4	3
9c	7	Crys–N	159	42.0	97
		N–I	161	1.4	3
9e	10	Crys–N	136	41.4	101
		N–I	153	1.2	3
9f	12	Crys–N	131	53.4	132
		N–I	145	1.1	3
9g	14	Crys–N	131	29.2	72.3
		N–I	142	0.9	2
11a	5	Crys–N	147	60.3	144
		N–I	177	1.2	3
11b	7	Crys–N	129	39.8	99
		N–I	171	1.3	3

Experimental

Characterization

Microanalyses were performed at Department of Chemistry, University of Sheffield, University of Exeter and Quantitative

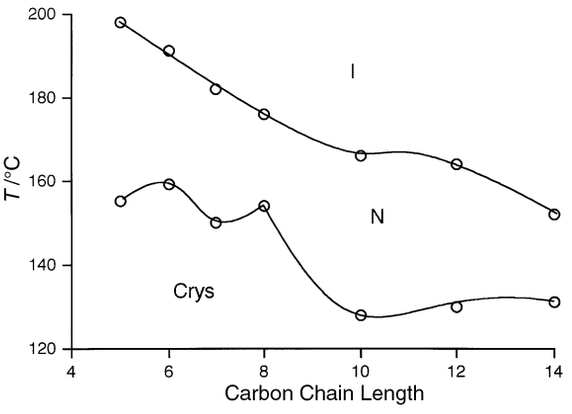

Fig. 11 Phase diagram for complexes **8**.

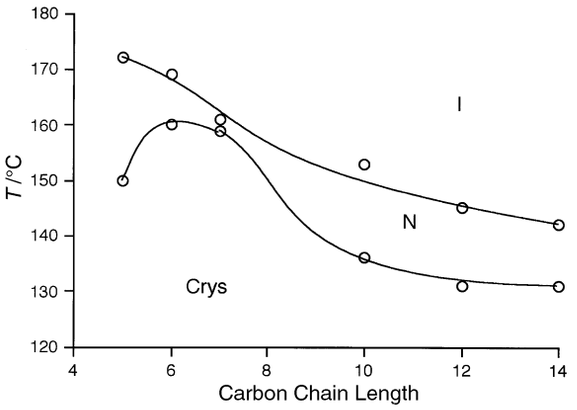

Fig. 12 Phase diagram for complexes **9**.

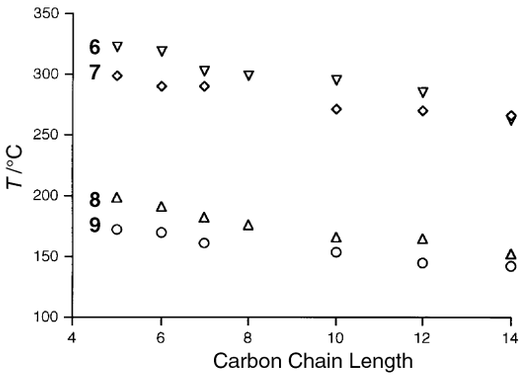

Fig. 13 Plot of clearing points for ligands **6** and **7** and complexes **8** and **9**.

Technologies Inc., Whitehouse, NJ, Microanalytical Service. All chemicals were used as received unless otherwise specified. Infrared spectra were recorded on a Perkin-Elmer 1600 FT infra-red spectrophotometer (4000–450 cm^{-1}) at University of Sheffield and a Nicolet Magna 550 IR spectrometer at University of Toronto. Spectra were recorded as Nujol mulls between polythene plates, or as CH_2Cl_2 solutions, or as KBr disks. ^1H and ^{13}C NMR spectra were recorded on a Bruker WM 250 and a Varian Gemini 200 spectrometer; chemical shifts are quoted relative to an internal deuterium lock. The melting points and phase transitions of liquid crystal materials were observed by differential scanning calorimetry (DSC) using a Perkin-Elmer DSC7 system with a Perkin-Elmer 7000 data station using TAS 7 software. Visual characterisation of the liquid-crystalline properties of the bulk materials was performed using a Zeiss Jenalab-pol polarising microscope equipped with a Linkam TH600 hot stage and PR600 temperature controller or a Mettler FP82 hot stage and FP80 central processor at University of Toronto.

Synthesis

All of the ligands and complexes were made using procedures which we have well documented elsewhere.[4,9] We therefore include only the analytical data for the new ligands (Table 4) and complexes (Table 5).

Table 4 Analytical data for the new ligands

		Calculated (Found)/%		
Compound	Yield (%)	C	H	N
6a	83.4	75.2 (75.6)	7.3 (7.1)	2.2 (2.2)
6b	85.6	75.3 (75.8)	7.2 (7.1)	2.2 (2.2)
6c	80.5	75.5 (76.0)	7.4 (7.4)	2.1 (2.1)
6d	83.4	75.9 (76.2)	7.7 (7.6)	2.0 (2.1)
6e	81.6	76.2 (76.6)	7.9 (7.9)	2.0 (2.0)
6f	75.4	76.5 (76.9)	8.1 (8.4)	1.9 (1.9)
6g	77.8	76.9 (77.2)	8.4 (8.3)	1.8 (1.8)
7a	86.4	76.1 (76.4)	7.7 (7.7)	2.0 (2.0)
7b	87.8	76.6 (76.6)	7.8 (7.9)	1.9 (2.0)
7c	82.3	76.7 (76.7)	8.0 (8.0)	1.9 (2.0)
7d	81.6	76.7 (77.2)	8.4 (8.3)	1.8 (1.9)
7e	76.4	77.5 (77.5)	8.6 (8.6)	1.7 (1.8)
7f	74.3	77.9 (77.8)	8.9 (8.8)	1.7 (1.7)
10a	81.4	77.0 (76.8)	8.5 (8.2)	2.3 (2.2)
10b	90.0	76.9 (77.1)	8.5 (8.5)	2.1 (2.1)

Table 5 Analytical data for the new complexes

		Calculated (Found)/%		
Compound	Yield (%)	C	H	N
8a	83.3	56.5 (56.6)	4.8 (4.8)	1.9 (1.5)
8b	81.5	57.0 (57.1)	5.0 (4.9)	1.5 (1.5)
8c	86.7	57.0 (57.5)	4.9 (5.0)	1.4 (1.5)
8d	83.3	57.6 (57.9)	5.0 (5.2)	1.7 (1.4)
8e	79.4	58.4 (58.7)	5.5 (5.4)	1.4 (1.4)
8f	74.5	59.1 (59.4)	5.6 (5.7)	1.4 (1.4)
8g	76.7	59.6 (60.1)	5.9 (5.9)	1.3 (1.3)
9a	87.4	57.8 (58.3)	5.3 (5.3)	1.4 (1.4)
9b	83.1	57.8 (58.6)	5.4 (5.4)	1.4 (1.4)
9c	78.9	58.4 (59.0)	5.6 (5.6)	1.4 (1.4)
9d	78.4	59.5 (60.1)	5.9 (5.9)	1.3 (1.3)
9e	73.2	60.3 (60.1)	6.1 (6.1)	1.3 (1.3)
9f	76.7	61.0 (61.4)	6.5 (6.3)	1.3 (1.3)
11a	73.2	57.4 (57.7)	5.4 (5.4)	1.5 (1.5)
11b	78.3	58.0 (58.1)	5.6 (5.7)	1.8 (1.5)

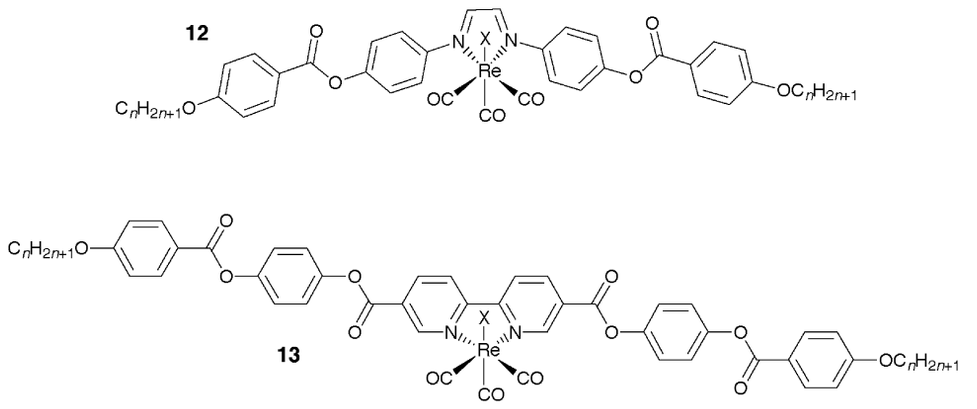

Fig. 14 Other mesomorphic complexes of octahedral Re(I).

Acknowledgements

The authors thank H. C. Stark for a generous gift of rhenium and X.H.L. thanks the University of Sheffield for a scholarship.

References

1 R. Deschenaux and J. Santiago, *J. Mater. Chem.*, 1993, **3**, 219; R. Deschenaux and J. Santiago, *Tetrahedron Lett.*, 1994, **35**, 2169; R. Deschenaux and J. W. Goodby, in *Ferrocenes*, ed. A. Togni and T. Hayashi, VCH, Weinheim, 1994, ch. 9, p. 471.
2 D. W. Bruce, *Adv. Mater.*, 1994, **6**, 699; D. W. Bruce, *J. Chem. Soc., Dalton Trans.*, 1993, 2983.
3 D. W. Bruce and X.-H. Liu, *J. Chem. Soc., Chem. Commun.*, 1994, 729.
4 D. W. Bruce and X.-H. Liu, *Liq. Cryst.*, 1995, **18**, 165; X.-H. Liu, M. N. Abser and D. W. Bruce, *J. Organomet. Chem.*, 1998, **551**, 271.
5 W. Beck and K. Raab, *Inorg. Synth.*, 1990, **28**, 15.
6 G. W. Gray and J. W. Goodby, *Smectic Liquid Crystals: Textures and Structures*, Leonard Hill, Glasgow, 1984.
7 S. Diele, D. Demus and H. Sackmann, *Mol. Cryst., Liq. Cryst.*, 1980, **56**, 217; J. J. Benattar, F. Moussa and M. Lambert, *J. Phys.*, 1981, **42**, L67; P. A. C. Gane, A. J. Leadbetter and P. G. Wrighton, *Mol. Cryst., Liq. Cryst.*, 1981, **66**, 247.
8 J. E. Maclennan and M. Seul, *Phys. Rev. Lett.*, 1992, **69**, 2082; C. Y. Chao, S. W. Hui, J. E. Maclennan, C. F. Chou and J. T. Ho, *Phys. Rev. Lett.*, 1997, **78**, 2581.
9 M.-A. Guillevic, M. J. Danks, S. K. Harries, S. R. Collinson, A. D. Pidwell and D. W. Bruce, *Polyhedron*, in press.
10 M.-A. Guillevic and D. W. Bruce, *Liq. Cryst.*, 2000, **27**, 153.
11 S. Morrone, G. Harrison and D. W. Bruce, *Adv. Mater.*, 1995, **7**, 665; S. Morrone, D. Guillon and D. W. Bruce, *Inorg. Chem.*, 1996, **35**, 7041.
12 K. E. Rowe and D. W. Bruce, *J. Chem. Soc., Dalton Trans.*, 1996, 3913; K. E. Rowe, PhD Thesis, University of Sheffield, 1997.

Paper a908137b